

CHARACTERIZATION OF CARBON NANOTUBES SYNTHESIZED FROM HYDROCARBON-RICH FLAME

Win Hon Tan¹, Siew Ling Lee², Jo-Han Ng^{3,4}, William Woei Fong Chong^{1,4}, Cheng Tung Chong^{1,4,*}

¹*Faculty of Mechanical Engineering, Universiti Teknologi Malaysia, 81310 Skudai, Johor, Malaysia*

²*Centre for Sustainable Nanomaterials, Ibnu Sina Institute for Scientific and Industrial Research, Universiti Teknologi Malaysia 81310 Skudai Johor, Malaysia*

³*Faculty of Engineering and the Environment, University of Southampton, Malaysia Campus (USMC), 79200 Nusajaya, Johor, Malaysia*

⁴*UTM Centre for Low Carbon Transport in cooperation with Imperial College London
Universiti Teknologi Malaysia, 81310 Skudai Johor, Malaysia*

(Received: October 2015 / Revised: December 2015 / Accepted: January 2016)

ABSTRACT

The present study focuses on the characterization of carbon nanotubes (CNTs) synthesized from flame under an atmospheric condition. A laminar flame burner was utilized to establish a rich premixed propane/air flame at the equivalence ratio $\phi = 1.8$ –2.2. The flame was impinged on a stainless steel wire mesh coated with nickel (Ni) catalyst to grow CNTs. Distribution and yield of the CNTs on the substrate were quantified. Carbon nanotubes formed on the substrate were harvested and characterized using scanning electron microscopy (SEM), field emission scanning electron microscopy (FESEM), energy dispersive X-ray spectroscopy (EDX), and thermogravimetric analysis (TGA). The FESEM micrograph showed that the CNTs produced were in disarray. The synthesized CNTs were an average of 50–60 nm in diameter while the length of the tubes was in the order of microns. TGA analysis showed that 75% of CNTs were present in the sample and the oxidation temperature was 510°C.

Keywords: Carbon nanotubes; FESEM; EDX; Flame synthesis; Nickel catalyst

1. INTRODUCTION

Carbon nanotubes (CNTs) are a promising material due to their outstanding properties. CNTs possess a mechanical strength 10 times greater than steel despite having a density one-sixth that of steel (Dresselhaus et al., 1996). Thus, CNTs provide good material reinforcement for low-density and high-strength composites. The demand for CNTs has continually increased due to their ability to improve existing applications. However, due to the high production cost of CNTs, their production rate is limited. Although methods such as chemical vapor deposition (CVD), laser ablation, or arc discharge can be used to produce CNTs, the production yield and setup costs can be prohibitive. Economical methods are needed to produce CNTs on a large scale to fulfill industry demands.

The combustion of hydrocarbon is an exothermic reaction that is capable of providing high-temperature medium-rich carbon radical suitable for CNT growth. Various hydrocarbon gases have been found to successfully produce CNTs. Rich premixed and diffusion flames have

*Corresponding author's email: ctchong@mail.fkm.utm.my, Tel. +607-5534631, Fax. +607-5566159
Permalink/DOI: <http://dx.doi.org/10.14716/ijtech.v7i2.3284>

shown the ability to synthesize CNTs (Gore & Sane, 2011). Premixed flame has an advantage over diffusion flame as it enables control of the mixture equivalence ratio and flame strength.

Several groups have performed studies on CNT synthesis using the premixed flame synthesis method. Vander Wal et al. (2002) synthesized CNTs using various premixed flames with different hydrocarbon sources, including ethane, ethylene, acetylene, and propane fuel-rich flame. CNTs were observed to grow in these cases. However, in cases using methane as a hydrocarbon source in the mixture with an equivalence ratio $\phi = 1.5\text{--}2.0$, no CNT growth was observed.

Height et al. (2004) conducted an experiment to study nanotubes' formation zone, growth time scale, transition conditions, and tube structure under different flame conditions. Single-walled CNT formation was observed using a premixed flame of acetylene/oxygen/15 mol % Ar at 6.7 kPa with Fe(CO) as a catalyst. An experiment performed by Woo et al. (2009) used a double-faced wall stagnation flow burner to study the formation of CNTs. Ethylene was used as a hydrocarbon fuel source, and two flows impinged on a flat stagnation wall where the substrate surfaces were coated with nickel. Despite successfully synthesizing CNTs, these experiments did not report on the quantities of CNTs produced.

Flame synthesis is an effective way to synthesize CNTs without large setup costs and huge energy inputs. This study focuses on using the premixed flame method to synthesize and characterize CNTs. Parametric studies were conducted to determine the optimum conditions for CNT production.

2. EXPERIMENTAL SETUP

Figure 1 shows the experimental setup for CNT synthesis. This experiment was performed using a premixed flame burner. The burner nozzle outlet was 20 mm in diameter, while the body inner tube diameter and height were 70 mm and 350 mm, respectively. Propane was used as the fuel source to generate a premixed rich flame, providing the carbon source for CNT growth. Two mass flow controllers with an accuracy of $\pm 1\%$ (Sierra; SmartTrack50) were used to control the mass flow rate of air and propane. A substrate (wire mesh) coated with nano-sized nickel catalyst was placed above the premixed burner to enable CNT growth. The substrate was held by an extended arm attached to a positioner. The distance between the burner nozzle outlet and the substrate, k , could be adjusted with the positioner. CNT yield was determined using a weighting method.

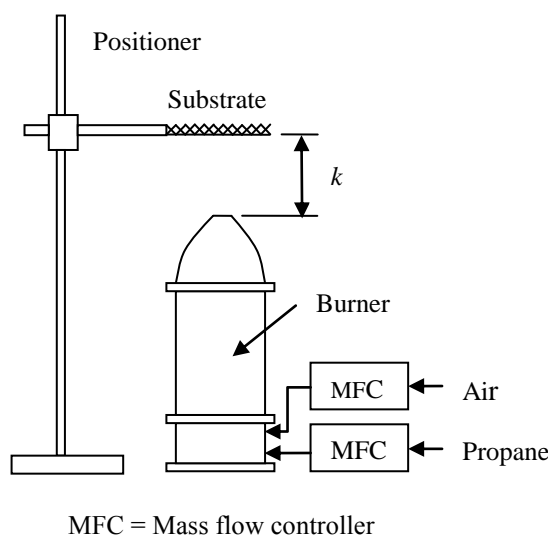


Figure 1 Schematic of experimental setup for production of CNTs

After the flame synthesis process, a layer of carbon was deposited on the substrates. The distribution of CNTs on substrates was observed using scanned electron microscopy (SEM). CNT powder was harvested from the substrate. The CNTs were purified by immersion in 30% H_2O_2 for 24 hours, followed by 22% HCl treatment for 24 hours (Datsyuk et al., 2008). Distilled water was used to rinse the CNTs until pH 7 was reached. The sample was analyzed using field emission scanning electron microscopy (FESEM) and energy dispersive X-ray spectroscopy (EDX). The impurity content, such as amorphous carbon, CNTs, and catalyst, was determined through thermogravimetric analysis (TGA) using air flow. The temperature range tested was from room temperature to 900°C at an incremental rate of 10°C/min.

Table 1 Parameters of experiment

Case	Fixed parameters	Variable parameters
1	Mesh number 60, $\phi = 2.2$, $t = 10$ min	Total air/propane
		a. 0.9 g/s
		b. 1.2 g/s
		c. 1.5 g/s
2	Mesh number 80, Total flow of air/propane = 1.2 g/s, $t = 10$ min	Equivalent ratio ϕ
		a. 1.8
		b. 2.0
		c. 2.2
3	Total flow of air/propane = 1.2 g/s, $\phi = 2.2$ and $t = 10$ min	Mesh number
		a. 60
		b. 80
		c. 100

Parametric studies were conducted to investigate the optimum operating conditions for CNT yields. Table 1 summarizes the operating conditions for all case tested.

3. RESULTS AND DISCUSSION

3.1. Distribution of CNTs on Mesh

Figure 2a shows the CNT-laden substrate (mesh number 40) after flame synthesis. Deposited carbon can be observed on the wire mesh in the area in contact with the flames. The location of the burnt region is 22–36 mm in radius from the center of the substrate marked y, as shown in Figure 2a. A high density of CNTs was observed in the area marked y, as shown in the micrograph in Figure 2c. The location x in Figure 2a, between 0 and 22 mm in radius, was not in contact with the flame reaction zone and thus contained no CNTs. Figure 2b shows the micrograph for region x, where only catalyst particles were observed. In the region marked z in Figure 2d (36–50 mm from the center point), no CNTs were observed. The micrograph shows that only nickel catalyst was present. This highlights that CNTs can only grow in substrate areas that are in contact with flames and where a reaction takes place.

CNTs were observed to grow on the surface of substrate impinged by the luminous premixed flame zone. In this region, the bluish flame that was established near the burner outlet was the main reaction zone where excited CH^* radicals were radiated. The main reaction zone is the region with the highest temperature in the flame, thus allowing the high diffusional rate of carbon into transition metal (catalyst) (Lee et al., 2001). Within the reaction zone, intermediate species such as CH_3 , C_2H_2 , and CH_2O became the available carbon radical sources for the growth of CNTs (Merchan-Merchan et al., 2002; Vandooren et al., 1992). Propane fuel underwent pyrolysis during reaction and cracked to become acetylene. The acetylene then reacted with other radicals to become polyacetylenes or polyacetylenic radicals. Through a

cyclization process, polycyclic aromatic hydrocarbon (PAH) was formed, which then stacked up as platelets to form CNTs in the presence of a catalyst. Without a catalyst, the PAH formed soot in an agglomerated form (Zabetta & Hupa, 2005).

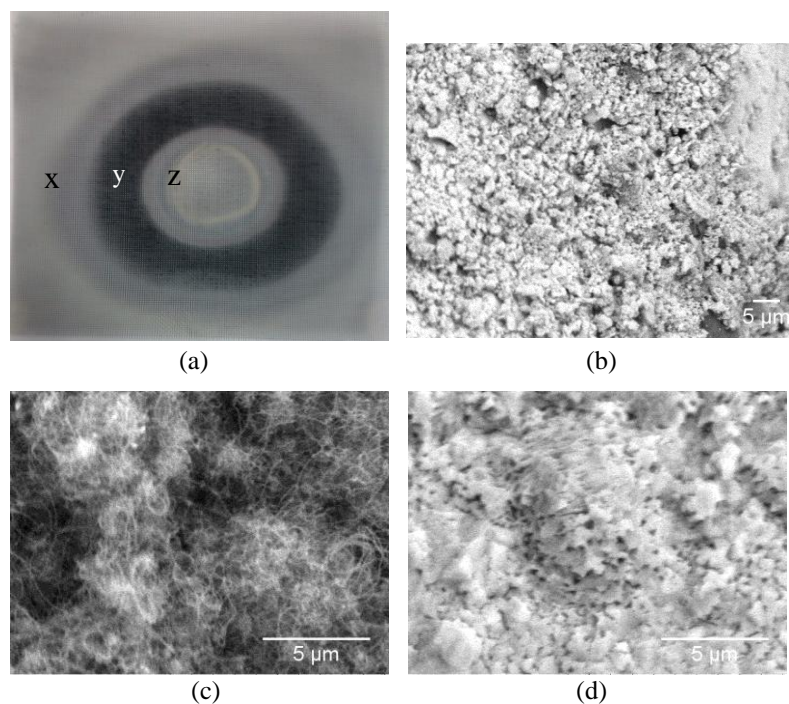


Figure 2 (a) Pictures of 10cm×10cm wire mesh after flame synthesis, SEM micrographs at (b) x-(c) y- and (d) z-labeled region

The region of 0–22 mm in radius (region z) is the pre-reaction flame zone. No reaction took place in this region and hence no carbon deposit was found on the substrate. In region x, no reaction took place as fuel was completely reacted with oxidizer in region y. Hence, no CNTs were observed in the former due the lack of carbon source.

3.2. FESEM Micrograph of CNT and EDX Analysis

Figures 3 shows the FESEM micrograph of nickel catalyst and untreated CNTs collected from substrates. Figure 3a shows the catalyst used for CNT synthesis, nano-scale nickel particles doped with alumina and silica. The nickel particle size ranged from 20–70 nm. Nickel has been reported to provide a higher growth rate of CNTs compared to iron and cobalt (Huang et al., 2002). Figures 3b, 3c, and 3d show the raw CNTs obtained at different magnification. In general, CNT growth was in disarray and in random directions. At higher magnification, particles were observed to deposit on the CNTs, as shown in Figure 3d. It was postulated that nickel was deposited on the CNTs. Previous studies showed that CNTs can be synthesized at temperatures between 700–900°C (Kumar & Ando, 2011). In the flame reaction zone, where the temperature could reach up to 2000°C, nickel, with a melting point of 1455°C, could melt and deposit onto the CNT surface, forming small particles during the process of flame synthesis. The fine nano-size nickel particles further induce melting due to the Gibbs–Thomson effect, where the melting temperature decreases as the particle size becomes smaller (Shibuta & Suzuki, 2010).

Figures 3c and 3d show that amorphous carbon was present in the untreated CNTs. From the FESEM micrograph, nickel catalyst was in the range of 28–60 nm (Figure 3a) while CNT ranged from 50–60 nm (Figure 3d). The present method typically produced CNTs within a diameter range of 50–60 nm, unperturbed by the catalyst size.

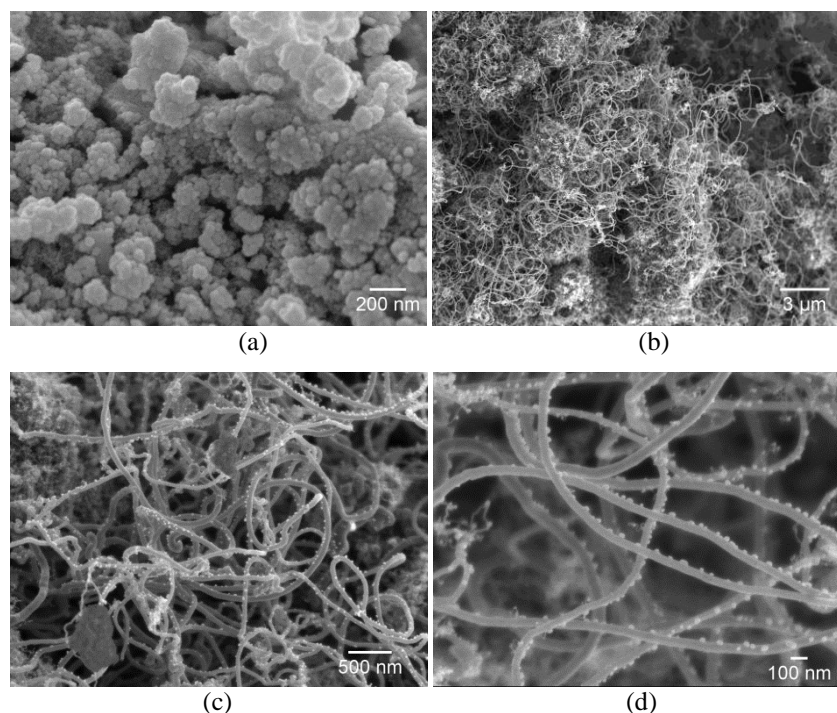


Figure 3 FESEM micrographs of: (a) nickel nanoparticle catalyst; (b) CNT cluster formed in disarray; (c) amorphous carbon present in CNT sample; and (d) CNT sample size measured in range of 50–60 nm

Figure 4 shows the EDX point analysis of the nickel particles deposited on the CNTs. The results confirm the high percentage of nickel present on the particles. EDX analysis was done on select area modes to identify the elements in the sample, and the results are shown in Table 2. There was a high mass percent of C 79.63%, and the elements Ni, O, Al, and Si were also detected, which originated from the catalyst (alumina and silica mixed with the nickel) used in this experiment.

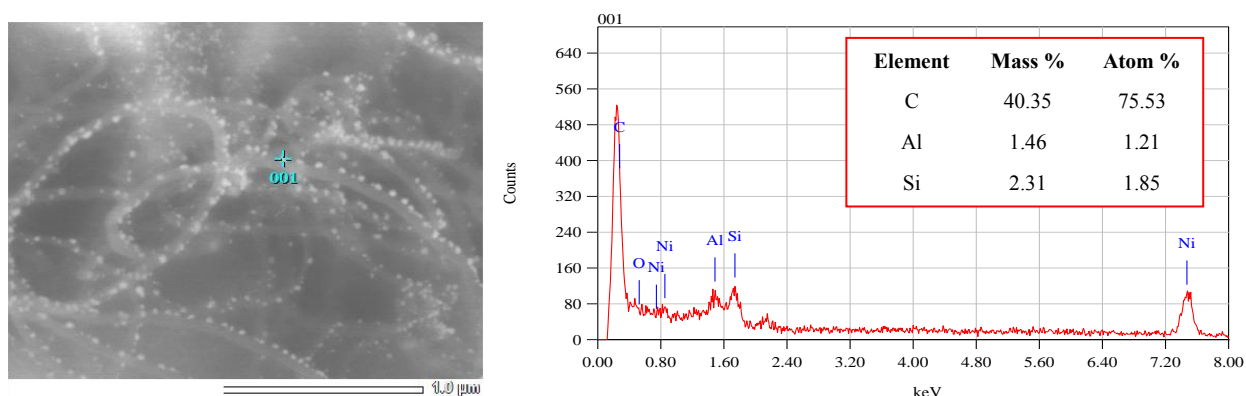


Figure 4 EDX analysis for the particle on the CNTs

Table 2 Quantitative analysis of the bulk sample on the CNTs

Element	Mass %	Atom %
C	79.629	89.134
O	9.615	8.080
Al	0.674	0.336
Si	0.567	0.271
Ni	9.515	2.179
Total	100.00	100.00

Total mass for the catalyst was 20.37%. This result is quite close to the TGA result for CNTs: 77% carbon content and 23% catalyst residual.

Figure 5 shows the FESEM micrograph of CNTs after purification treatment. The CNTs were cleared of nickel particle contamination by treatment with HCl acid. The aqueous solution acquired a yellowish and greenish color due to the presence of $[\text{NiCl}_4]^{2-}$ in the solution (Gill et al., 1967). Amorphous carbon can still be observed in the sample. H_2O_2 treatment needs to be applied longer to obtain CNTs with higher purity.

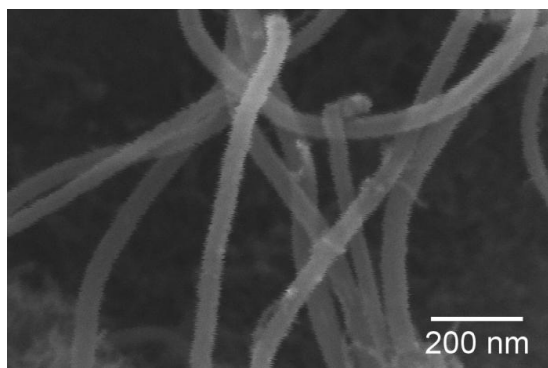


Figure 5 CNTs after purification treatment

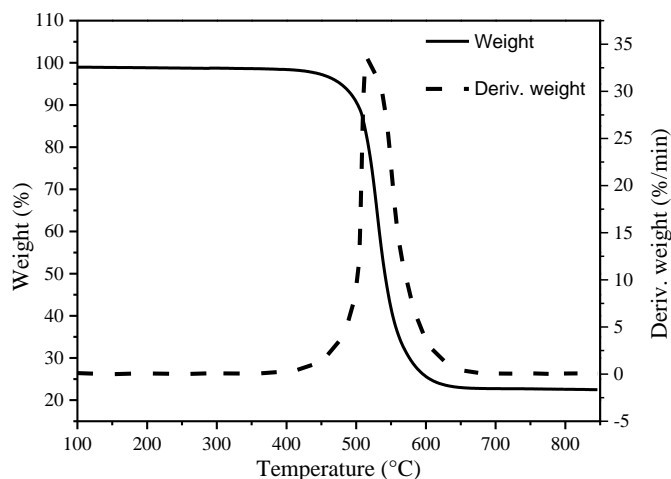


Figure 6 TGA result of CNT sample obtained experimentally

3.3. TGA Analysis

Thermogravimetric analysis (TGA) was used to analyze the thermal stability of the sample. Thermal stability is a good indicator of the overall quality of CNTs obtained. A higher oxidation temperature indicates that a sample has high purity. Carbon has different oxidation temperatures depending on the level of graphitized structure. Oxidation temperatures can be divided into three stages. At temperatures lower than 350°C, weight loss on the sample is due to water content and adsorbed species. At temperatures between 350°C and 400°C, amorphous carbon and disordered carbon start to oxidize. Above 400°C, oxidation of amorphous carbon and CNTs occurs simultaneously (Kumar, 2012).

Figure 6 shows the TGA result of CNTs obtained experimentally. CNTs began to gasify at around 400°C. The main weight loss was in the range of 400–650°C. Oxidation occurred at around 510°C while maximum weight loss occurred at 516°C. The rate of weight loss was 33.46%/min. The TGA result shows that weight loss before 400°C was relative small. This indicates that the CNT sample contained a high degree of crystalline perfection. When the temperature increased to 400°C, only a small portion (1.6%) of the sample was gasified. A residue content of about 23% was left after 650°C. The residue included alumina, silica, and nickel from the catalyst. These materials are relatively stable in air. The obtained result was similar to the other research CNT sample produced with the CVD method at 850°C (Lee et al., 2001).

3.4. CNT Yield

3.4.1. Effect of distance between substrate and burner outlet

Parametric studies were performed to study the optimum operating conditions for obtaining CNTs. Figure 7 shows the result of carbon yield as a function of distance between substrates and burner nozzle outlet, k . The mesh number of the substrate used was 60. The equivalence

ratio of the mixture was fixed at $\phi = 2.2$. The duration of the flame synthesis process for each test case was 10 min. The result shows that carbon yields increased as k increased until reaching a maximum point before decreasing. Maximum CNT yields for 0.9 g/s and 1.2 g/s of total air/propane mixtures were 0.11g. When the flow of air/propane increased to 1.5 g/s, the maximum carbon yield was about 0.09 g. An increase in air/propane flow from 0.9 g/s to 1.2 g/s did not result in an increase of carbon yield. Further increase of the air/propane flow rate to 1.5 g/s resulted in a drop in carbon yield. One would expect that increased air/propane flow would result in increased carbon yield. However, in the present experiment, a higher total mass flow rate of the air/propane mixture means higher flow velocity at the burner outlet. The high velocity of the reactants shortens the time for carbon radicals to diffuse into the catalyst to form CNTs, thus resulting in a decreased carbon yield.

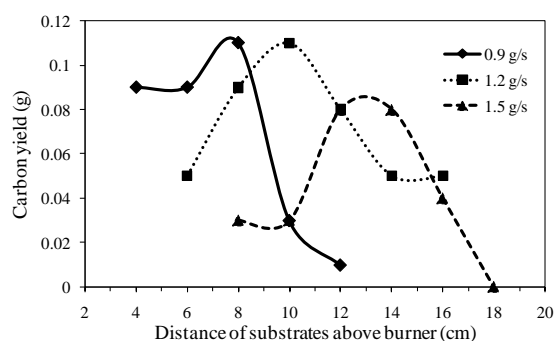


Figure 7 Effect of varied total propane/air mass flow rate on carbon yield as a function of distance between substrate and burner outlet. The wire mesh number was 60, the equivalent ratio of the mixtures was $\phi = 2.2$ while the synthesis process was $t = 10$ min

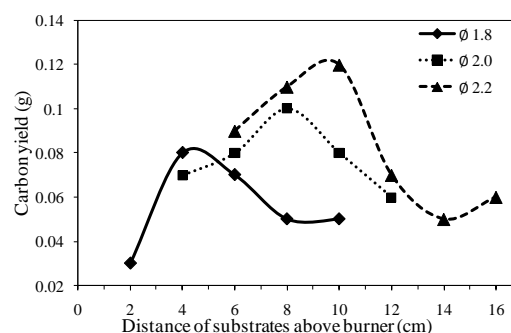


Figure 8 Effect of varied equivalence ratio ϕ on carbon yield as a function of the distance between the substrate and burner outlet. The mass flow of air/propane was fixed at 1.2 g/s. The flame synthesis process duration was $t = 10$ min

The peak carbon yields for total air/propane flow rates of 0.9, 1.2, and 1.5 g/s were located at $k = 8, 10$, and 13 cm, respectively. The difference in k is due to the fact that rich propane fuel diminishes the available oxygen for fuel, decomposing radicals and causing them to traverse a farther distance for better mixing (Kashir *et al.*, 2012). Carbon yield peaks when number of carbon radicals produced from pyrolysis of fuel is maximum. Carbon yield decreases when a large portion of the propane reacts with oxygen and completes the reaction into stable CO_2 and H_2O .

3.4.2. Effect of equivalence ratio

Figure 8 shows the carbon yield as a function of the distance of substrates above the burner at varied equivalent ratios of $\phi = 1.8, 2.0$, and 2.2 . The mesh number for the substrate used was 80, while the total flow rate of air/propane was fixed at 1.2 g/s. Higher carbon yield was obtained with richer flame due to the higher amount of carbon source available for CNTs growth. A flame with an equivalent ratio of $\phi = 2.2$ produces a maximum of 0.12 g of carbon at $k = 10$ cm. When the flame becomes richer, the highest yield of CNTs was obtained at a higher substrate position above the burner outlet. The peak CNT yield for $\phi = 1.8$ and $\phi = 2.0$ occurs when $k = 4$ cm and 8 cm, respectively. For a mixture with lower equivalence ratio (i.e., $\phi = 1.8$), a higher flame propagation rate results in a shorter flame. Fuel/air reactants travel a shorter distance to be fed into the reaction zone of the flame, thus resulting in a shorter distance for peak carbon yield.

3.4.3. Effect of substrate mesh size

The effect of mesh size on carbon yield was investigated. Figure 9 shows carbon yield as a function of the distance between the substrate and burner outlet. Three mesh sizes were used for the substrate: mesh number 60, 80, and 100. The flow of air/propane was fixed at 1.2 g/s, equivalent ratio $\phi = 2.2$, and $t = 10$ min. Stainless steel wire mesh with a mesh number of 80 resulted in a higher yield of carbon compared to the other two types of mesh within 10 cm above the burner with a maximum carbon yield of 0.12 g. The lowest yield of carbon was found with the wire mesh of mesh number 100, with the maximum carbon yield of 0.08 g obtained at the distance $k = 8$ cm above the burner.

Although a larger mesh number means a larger surface area, mesh with a mesh number of 100 resulted in the lowest yield. This is because the gaps for mesh number 100 are too fine and restricted flow through the mesh. Mesh number 60 showed a lower yield for $k < 10$ cm but similar yield for $10 \text{ cm} < k < 16$ cm compared to mesh number of 80.

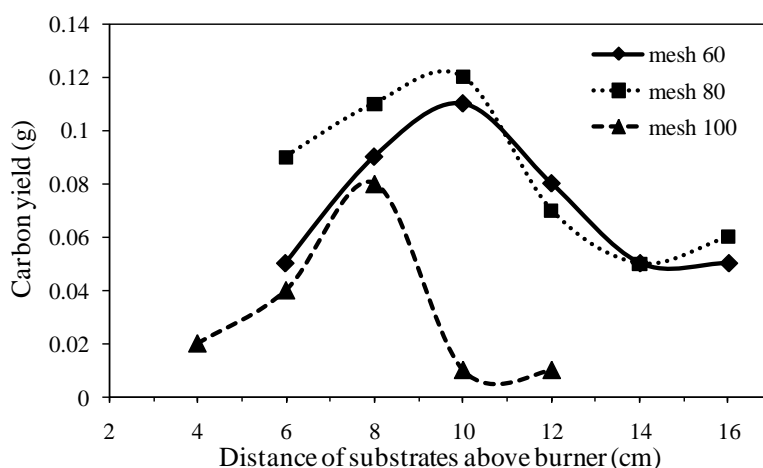


Figure 9 Effect of mesh size on carbon yield as a function of the distance between the substrate and burner outlet. The total mass flow rate of air/propane was 1.2 g/s with the equivalent ratio of $\phi = 2.2$. The flame synthesis process was $t = 10$ min

4. CONCLUSION

Flame synthesis has been utilized to produce CNTs. The CNTs grown on substrates were in disarray, with nickel particles deposited on the surface. The synthesized CNTs showed an average diameter of 50–60 nm. TGA analysis results indicate that treated CNT samples contained 75.4% purity of CNTs. CNTs produced by flame synthesis showed thermal stability of around 510°C. From the parametric studies, substrate with mesh number 80 at a distance of 10 cm from the burner outlet, total air/propane flow rate of 1.2 g/s at $\Phi=2.2$ can produce a high yield of CNTs under 10 minutes of flame synthesis process.

5. ACKNOWLEDGEMENT

The financial support of the Ministry of Higher Education Malaysia and Universiti Teknologi Malaysia (Research university grant Tier-1 vot no.: 09H79) is gratefully acknowledged.

6. REFERENCES

- Datsyuk, V., Kalyva, M., Papagelis, K., Parthenios, J., Tasis, D., Siokou, A., Kallitsis, I., Galiotis, C., 2008. Chemical Oxidation of Multiwalled Carbon Nanotubes. *Carbon*, Volume 46(6), pp. 833–840

- Dresselhaus, M.S., Dresselhaus, G., Eklund, P.C., 1996. *Science of Fullerenes and Carbon Nanotubes: Their Properties and Applications*. Academic Press
- Gill, N.S., Taylor, F., Hatfield, W., Parker, W., Fountain, C.S., Bunger, F.L., 1967. Tetrahalo Complexes of Dipositive Metals in the First Transition Series. *Inorganic Syntheses*, Volume 9, pp. 136–142
- Gore, J.P., Sane, A., 2011. Flame Synthesis of Carbon Nanotubes. *Carbon Nanotubes-Synthesis, Characterization, Applications*, InTech, pp. 122–132
- Height, M.J., Howard, J.B., Tester, J.W., Vander Sande, J.B., 2004. Flame Synthesis of Single-Walled Carbon Nanotubes. *Carbon*, Volume 42(11), pp. 2295–2307
- Huang, Z., Wang, D., Wen, J., Sennett, M., Gibson, H., Ren, Z., 2002. Effect of Nickel, Iron, and Cobalt on Growth of Aligned Carbon Nanotubes. *Applied Physics A*, Volume 74(3), pp. 387–391
- Kashir, B., Tabejamaat, S., Baig, M.M. 2012. Experimental Study on Propane/Oxygen and Natural Gas/Oxygen Laminar Diffusion Flames in Diluting and Preheating Conditions. *Thermal Science*, Volume 16(4), pp. 1043–1053
- Kumar, C.S., 2012. *Raman Spectroscopy for Nanomaterials Characterization*: Springer Science & Business Media
- Kumar, M., Ando, Y., 2011. *Carbon Nanotube Synthesis and Growth Mechanism*: InTech, Open Access Publisher
- Lee, C.J., Park, J., Huh, Y., Lee, J.Y., 2001. Temperature Effect on the Growth of Carbon Nanotubes using Thermal Chemical Vapor Deposition. *Chemical Physics Letters*, Volume 343(1), pp. 33–38
- Merchan-Merchan, W., Saveliev, A., Kennedy, L.A., Fridman, A., 2002. Formation of Carbon Nanotubes in Counter-Flow, Oxy-Methane Diffusion Flames without Catalysts. *Chemical Physics Letters*, Volume 354(1), pp. 20–24
- Shibuta, Y., Suzuki, T., 2010. Melting and Solidification Point of Fcc-metal Nanoparticles with Respect to Particle Size: A Molecular Dynamics Study. *Chemical Physics Letters*, Volume 498(4), pp. 323–327
- Vander Wal, R.L., Hall, L.J., Berger, G.M., 2002. Optimization of Flame Synthesis for Carbon Nanotubes using Supported Catalyst. *The Journal of Physical Chemistry B*, Volume 106(51), pp. 13122–13132
- Vandooren, J., Branch, M., Van Tiggelen, P., 1992. Comparisons of the Structure of Stoichiometric $\text{CH}_4\text{-N}_2\text{O-Ar}$ and $\text{CH}_4\text{-O}_2\text{-Ar}$ Flames by Molecular Beam Sampling and Mass Spectrometric Analysis. *Combustion and Flame*, Volume 90(3), pp. 247–258
- Woo, S., Hong, Y., Kwon, O., 2009. Flame-synthesis Limits and Self-catalytic Behavior of Carbon Nanotubes using a Double-faced Wall Stagnation Flow Burner. *Combustion and Flame*, Volume 156(10), pp. 1983–1992
- Zabetta, E.C., Hupa, M., 2005. Gas-born Carbon Particles Generated by Combustion: A Review on the Formation and Relevance. *Combustion and Materials Chemistry*. ABO AKADEMI, FIN-20500 Åbo, Finland